The following publication K. Qu, Y. Gu, Z. Zang, A. Chen and X. Xu, "Modeling the Non-Identical Perception Variance in Day-to-Day Dynamics via Weibit-Based Network Loading Function," in IEEE Transactions on Intelligent Transportation Systems, vol. 26, no. 7, pp. 10968-10978, July 2025 is available at https://doi.org/10.1109/TITS.2025.3556380.

Modeling the Non-Identical Perception Variance in Day-to-Day Dynamics via Weibit-Based Network Loading Function

Kai Qu, Yu Gu, Zhaoqi Zang, Anthony Chen, Xiangdong Xu

***Abstract*—The Weibit choice model has gained increasing attention in transportation studies. Compared with the commonly used Logit model, the Weibit model inherently captures the heterogeneous travel perceptions by allowing non-identical variances for different alternatives. Nevertheless, how travelers' heterogeneous perception errors may influence day-to-day (DTD) network dynamics, in which route choice decisions are made on each day, remains underexplored. In this study, we present several deterministic discrete DTD dynamic traffic models with Weibit-based network loading function, termed Weibit-based DTD dynamic models. We provide the asymptotic stability conditions of the Weibit stochastic equilibrium states based on the Jacobian matrices of the dynamical systems. We demonstrate how the features of non-identical perception variances and asymmetric response curve of the Weibit model can influence the evolution of network states and eventually the equilibrium points of the dynamical systems compared to the Logit case. Under fair comparison, the equilibrium states of Weibit DTD models are shown to have larger stable regions of adjustment rates than those of Logit DTD models. This research contributes to understanding the significance of considering travelers' non-identical perception errors in DTD dynamics.**

***Index Terms*—Day-to-day; stability; Weibit; travel choice model; traffic assignment.**

I. Introduction

A. Background

DYNAMICS in transportation networks have received great attention as a complement to the commonly studied network equilibrium state. Understanding the day-to-day (DTD) evolution of traffic flows is crucial for designing or refining network operation and management strategies (e.g., dynamic signal control [1], dynamic pricing of tradable mobility credits or transportation network company services [2], [3], and dynamic congestion pricing schemes [4]).

DTD models have been extensively studied in the literature. This study focuses on DTD models with stochastic user equilibrium (SUE) as the fixed point, which is different from the user equilibrium (UE, [5], [6]) due to the consideration of travelers' perception error. [7] first studied the DTD dynamics of a stochastic equilibrium in a two-link transportation network where the perceived cost is the sum of the measured cost and a random variable. [8] studied the stability of Logit stochastic equilibrium in general transportation networks. [9] further investigated the case of non-monotone cost functions. [10] estimated the attraction domains of SUE states. [11] proposed a discrete rational adjustment process to formulate the evolution of link flows and discussed the case of having SUE as the fixed point. [12] proposed an extended proportional-switch adjustment process model. [13] established a general framework for continuous DTD models to capture the perceptual errors. [14] studied the DTD dynamical system under advanced traveler information and showed that the discrete-time and continuous-time models have large differences in stability conditions. [15] explored the interconnection between several classical types of continuous DTD models with SUE states as fixed points.

The above studies are mostly the Logit-based DTD models with Logit-based network loading function. Logit model has been widely used since it allows the closed-form probability expression due to the underlying Gumbel distribution of travelers' perception errors ([16], [17]). However, the error is assumed to be independently and identically distributed (IID). The independently distributed assumption makes it impossible to consider the similarity between travel alternatives, and the identically distributed assumption makes it impossible to consider alternative-specific perception variances of travel alternatives. To relax the identically distributed assumption, [18] proposed and derived the Weibit choice model based on the Weibull distribution of perception error. The Weibit model also has the closed-form probability expression which enables the efficient probability computation. [19], [20] developed the Weibit-SUE model. Existing studies have empirically validated the effectiveness of Weibit-based choice models. [21] found that the multiplicative error structure (e.g., Weibit model), which evaluates relative differences in utility, often outperformed traditional additive utility functions (e.g., Logit models). Further real-world calibration in route choice, travel mode selection, and railway itinerary choice have confirmed their superiority (e.g., [22]–[24]). Due to the ability to capture the non-identical variances for different alternatives, the Weibit model has received increasing attention, including the traffic equilibrium problems ([19], [20], [25]), the mode choice problems ([26], [27]), facility location problems ([28]), train

This paper is supported by the Research Grants Council of the Hong Kong Special Administrative Region (PolyU 15222221) and National Natural Science Foundation of China (72331001) (*Corresponding author: Anthony Chen, e-mail: anthony.chen@polyu.edu.hk*)

Kai Qu is with the Department of Civil and Environmental Engineering, the Hong Kong Polytechnic University, and Urban Mobility Institute, Tongji University China. (e-mail: kkkai.qu@connect.polyu.hk). Yu Gu, and Anthony Chen are with the Department of Civil and Environmental Engineering, the Hong Kong Polytechnic University, China (e-mail: frank.gu@connect.polyu.hk, anthony.chen@polyu.edu.hk). Zhaoqi Zang is with the School of Civil and Environmental Engineering, Nanyang Technological University, Singapore (e-mail: zhaoqi.zang@ntu.edu.sg). Xiangdong Xu is with the Urban Mobility Institute, College of Transportation Engineering, Tongji University, Shanghai, China. (e-mail: xiangdongxu@tongji.edu.cn).

scheduling problems ([29]), and congestion pricing problems ([30]). However, Weibit model is rarely explored in the context of DTD dynamics which involves travelers' choice from one day to another. Although [31] and [30] applied Weibit-based DTD models to congestion pricing and network vulnerability problems, they did not uncover in detail the model properties (e.g., the stability, concerned with whether the dynamic adjustments will ultimately reach the equilibrium).

B. Research gap, objective, and contribution

From the above discussion and the summary in Table I, while the Weibit model has received some attention in the literature, most of them focus on static problems rather than dynamic settings. None has explored the features of the Weibit model in the context of DTD dynamics in detail. To fill this research gap, this study theoretically establishes stability conditions for discrete-time Weibit DTD models and explicitly compares them to Logit DTD models across various networks and settings through extensive numerical experiments. Additionally, this study details how the non-identical variance feature influences network state evolution and presents the asymmetric response curve feature in DTD dynamics for the first time. The applicability to the realistic network is demonstrated. Insights are also discussed.

TABLE I: A selective summary of literature on DTD dynamics and choice modeling in the transportation field

Literature	DTD	Stability	Logit	Weibit	Weibit feature
[16], [17]			✓		
[7]–[10], [12]–[14], [32]	✓	✓	✓		
[18]–[20]				✓	✓
[30], [31]	✓			✓	
[15]	✓	✓	✓	✓	
This study	✓	✓		✓	✓

Note: [15] did not explicitly compare the stability region of Logit and Weibit DTD models.

The remainder of this study is organized as follows. Section II presents the methodology. Section III presents numerical examples. Section IV presents the summary and future research directions.

II. METHODOLOGY

A. Review of the Logit and Weibit route choice models

1) Logit route choice model: The multinomial Logit (MNL) route choice probability is given by ([16]),

$$prob_{w,r}^{Logit}(\mathbf{c}_w) = \frac{e^{-\theta c_{w,r}}}{\sum_{l \in R^w} e^{-\theta c_{w,l}}}, \forall r \in R^w, w \in W \quad (1)$$

where $prob_{w,r}^{Logit}$ is the Logit probability of selecting route r that connects O-D pair w belonging to the set of O-D pairs W, $\mathbf{c}_w = \{c_{w,1}, \ldots, c_{w,l}\}$ is the vector of path costs for O-D pair w. θ is the Logit dispersion parameter. R^w is the set of paths that connect the O-D pair w. The path cost is typically assumed to be the sum of the link costs, i.e., $\mathbf{c}_{w,r} = \sum_{x \in L_{w,r}} c_x$, where c_x is the link cost (travel time in this paper), and $L_{w,r}$ is the set of links on the route r that connects O-D pair w. Logit model has two known drawbacks: (i) inability to account for overlapping (or correlation) among routes, and (ii) failure to account for perception variance with respect to trips of different lengths [33]. The perception variance in the Logit model is constant among alternatives at $(\sigma_{w,r})^2 = \frac{\pi^2}{6\theta^2}$.

2) Weibit route choice model: The multinomial Weibit (MNW) route choice probability is given by ([18]),

$$prob_{w,r}^{Weibit}(\mathbf{g}_w) = \frac{(g_{w,r})^{-\beta_w}}{\sum_{l \in R^w} (g_{w,l})^{-\beta_w}}, \forall r \in R^w,\ w \in W \quad (2)$$

where $prob_{w,r}^{Weibit}$ is the probability of selecting route r that connects O-D pair w under the Weibit model, $\mathbf{g}_w = \{g_{w,1}, \ldots, g_{w,l}\}$ is the vector of path costs for O-D pair w in the Weibit model, and β^w is the shape parameter. The perception variance is route-specific, which is given by $(\sigma_{w,r})^2 = \left[\frac{g_{w,r}}{\Gamma(1+\frac{1}{\beta^w})}\right]^2 \left[\Gamma\left(1+\frac{2}{\beta^w}\right) - \Gamma^2\left(1+\frac{1}{\beta^w}\right)\right]$, where $\Gamma(\cdot)$ is the Gamma function.

However, the feature of non-identical variances is rarely explored in detail in the context of DTD dynamics. In a DTD dynamic transportation network, as travel costs — whether actual or predicted — fluctuate daily, the perceived variance for the costs of different routes may also vary by day correspondingly. To illustrate identical and non-identical perception variance, consider a two-route network where the cost of route 1 rises from 3 to 5, and the cost of route 2 drops from 8 to 6 over three days. Fig. 1 shows the perceived cost distribution captured by the two models under $\theta = 1$ and $\beta^w = 3.7$. It can be observed that the Weibit model captures the varying perception variances across routes, while the Logit model keeps cost variances constant despite DTD changes. Note that in reality travelers may perceive errors differently for routes with varying costs [33]. In DTD dynamics, this can affect the evolution of network flow, costs, and potentially the stability of the dynamical system as demonstrated later.

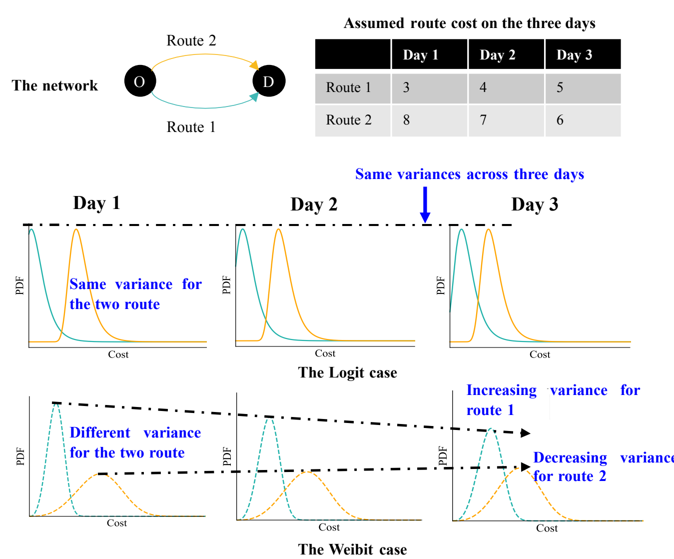

Fig. 1: Illustration of the identical (Logit) and non-identical (Weibit) perception variances in DTD dynamics

B. Weibit-based DTD models and stability conditions

DTD models can be categorized into *deterministic models versus stochastic models, and discrete models versus continuous models* (see [2]). The DTD models in this research are deterministic discrete models. Deterministic models are more commonly studied in the literature, and can be deemed as an approximation of the stochastic models (e.g., [34], [35]). On the other hand, discrete models can better represent the reality, and their stability conditions are more complex than continuous models (see [14]).

Depending on the explicitly modeled state variables, DTD models can be further categorized into *flow dynamic model* (with flow as the state variables, e.g., [11], [31], [32], [36]–[39], *cost dynamic model* (with cost as the state variables, e.g., [7], [9], [10], [13] and *double dynamic model* (with both flow and cost as the state variables, e.g., [8], [14], [30], [40]. Below we present three types of deterministic discrete DTD models under Weibit-based network loading functions (called Weibit-based DTD models) as well as the important local asymptotic stability conditions of the equilibrium points.

Remark 1. We focus on the local asymptotic stability instead of the global stability (see the definition of stability in [15]). The reason is that the local asymptotic stability of the discrete-time models allows for explicitly determining the critical rates of adjustment (related to the flow adjustment process or/and learning process) of the equilibrium states used to compare the Weibit and Logit DTD models. Note that [15] demonstrated the global stability of continuous-time Weibit-based DTD models by constructing the Lyapunov functions and referring to the LaSalle's Theorem, but they did not explicitly compare the stability regions of Weibit and Logit DTD models. In addition, we assume that all involved functions are continuous (i.e., travel time functions and network loading functions), which is a mild assumption and ensures the fixed-point existence.

1) Flow-based dynamic model: Flow dynamic models formulate the dynamics of flows as the functions of flows and costs. For the Weibit-based flow dynamic model, the flow adjustment process is given by,

$$\mathbf{f}^{k+1} = \alpha \Phi^{Weibit}(\mathbf{g}(\mathbf{f}^k)) + (1-\alpha)\mathbf{f}^k \tag{3}$$

where $\mathbf{f}^k = \{\mathbf{f}^{k,1}, \mathbf{f}^{k,2}, \ldots, \mathbf{f}^{k,w}\}$ with $\mathbf{f}^{k,w} = \{f_1^{k,w}, f_2^{k,w}, \ldots, f_r^{k,w}\}$ is the route flow vector, $f_r^{k,w}$ indicating the route flow of route r that connects O-D pair w on day k; $\Phi^{Weibit}(\cdot)$ is the Weibit-based network loading function, which determines the target route flow of the next day given previous days' route cost, i.e.,

$$\Phi_{w,r}^{Weibit}(\mathbf{g}_w) = q_w * prob_{w,r}^{Weibit}(\mathbf{g}_w), \quad \forall w \in W, r \in R_w \tag{4}$$

where q_w is the travel demand of O-D pair w. Eq. (3) states that the path flow on one day is a weighted combination of the target flow of that day and the path flow of the previous day, where α is the flow adjustment ratio reflecting the percentage of travelers adjusting their routes. For the Logit case, the difference lies in that the loading function is Logit-based loading function ([11], [32]).

Equivalence condition 1. *The fixed point of the dynamical system (3) + (4) is equivalent to the Weibit-SUE.*

Proof. See Appendix-A1. □

Proposition 1. *For the dynamical system (3) + (4), the equilibrium point is stable when $\mu_{\min} > 1 - \frac{2}{\alpha}$, where $\mu_{\min}$ is the minimum eigenvalue of the matrix $J_g^{\Phi^{Weibit}} J_f^g$ for the Weibit-based model (i.e., $\mu_{\min} := \min_{i=1,2,\ldots,N} \mu_i$, where N is the total number of paths). Here $J_g^{\Phi^{Weibit}}$ means the Jacobian matrix of the Weibit network loading function with respect to the path cost, and J_f^g means the Jacobian matrix of the path cost with respect to the path flow.*

Proof. See Appendix-B1. □

2) Cost dynamic model: Cost dynamic models formulate the dynamics of costs as the functions of flows and costs. The flow on each day is determined by the predicted cost denoted by $\mathbf{p}$ via the network loading function. For the Weibit case, in the learning process, the logarithm of the predicted path cost follows the exponential smoothing ([15], [19], [20]) due to the multiplicative cost structure, i.e.,

$$\ln \mathbf{p}^{k+1} = \gamma \ln \mathbf{g}^k(\mathbf{f}^k) + (1-\gamma)\ln\mathbf{p}^k \tag{5}$$

where γ is the learning parameter. The Weibit-based network loading is given by,

$$\mathbf{f}^k = \Phi^{Weibit}(\mathbf{p}^k) \tag{6}$$

For Logit-based cost dynamic model, the difference lies in twofold: First, the network loading function is the Logit-based function; second, there is no logarithm function in the cost term in Eq. (5) (see [9], [10], [15]), i.e., the learning process is given by $\mathbf{p}^{k+1} = \gamma \mathbf{c}^k(\mathbf{f}^k) + (1-\gamma)\mathbf{p}^k$.

Equivalence condition 2. *The fixed point of the dynamical system (5) + (6) is equivalent to the Weibit-SUE.*

Proof. See Appendix-A2. □

Proposition 2. *For the dynamical system given by (5) + (6), the equilibrium point is stable when $\mu_{\min} > 1 - \frac{2}{\gamma}$, where $\mu_{\min}$ is the minimum eigenvalue of the matrix $J_g^{\Phi^{Weibit}} J_f^g$ for the Weibit-based model.*

Proof. See Appendix-B2. □

3) Double dynamic model: Some DTD models capture both the dynamics of flows via the flow adjustment process and the dynamics of costs via the learning process (e.g., [8]). We call such models the double dynamic models. In the Weibit case, the double dynamic model is given by (7) + (8) as follows,

$$\mathbf{f}^{k+1} = \alpha \Phi^{Weibit}\left(\mathbf{p}(\mathbf{f}^k)\right) + (1-\alpha)\mathbf{f}^k \tag{7}$$

$$\ln \mathbf{p}^{k+1} = \gamma \ln \mathbf{g}^k(\mathbf{f}^k) + (1-\gamma)\ln \mathbf{p}^k \tag{8}$$

Equivalence condition 3. *The fixed point of the dynamical system (7) + (8) is equivalent to the Weibit-SUE.*

Proof. See Appendix-A3. □

Proposition 3. *An equilibrium point of the dynamical system given by (7) + (8) is stable when $\mu_{min} > -2\frac{(1-\gamma)+(1-\alpha)}{\alpha\gamma} - 1$,, where μ_{min} is the minimum eigenvalue of the matrix*

$J_g^{\Phi^{Weibit}} G J_f^{\ln g}$, *where* G *is a diagonal matrix given by* $G = diag(g_1, g_2, \ldots, g_N)$.

Proof. See Appendix-B3. □

4) Summary and critical rate of adjustment: It is shown that the above DTD dynamic models will have Weibit-SUE as the fixed point. Also, **Propositions 1 to 3** state the stability conditions. Like many existing studies, the adjustment rates α and γ are assumed to be fixed. By slight manipulation, we may accordingly define a critical parameter (or critical parameter combination) to determine whether an equilibrium point is stable or not under a given rate of adjustment (i.e., α, γ or the combination of the two). Such critical parameter (or combination) can determine the stable region used for comparing the stability condition of the equilibrium states of Weibit and Logit-based DTD models. Specifically, we present the following two definitions.

Definition 1. (Critical α in the flow dynamic model). For the flow dynamic model, by simple manipulation of Proposition 1, we can obtain the relationship between the critical α and minimum eigenvalue μ_{min} given by $\alpha_{\text{critical}} = \frac{2}{1-\mu_{\text{min}}}$. That is, if $\alpha > \alpha_{\text{critical}}$, the equilibrium point is unstable and vice versa.

Note that we can similarly define a critical γ for the cost dynamic model as $\gamma_{\text{critical}} = \frac{2}{1-\mu_{\text{min}}}$.

Definition 2. (Critical γ versus critical α in the double dynamic model). For the double dynamic model, by simple manipulation of Proposition 3, we can obtain the relationship between the critical α, γ, and minimum eigenvalue μ_{min} given by $\gamma_{\text{critical}} = \frac{4-2\alpha_{\text{critical}}}{2-\alpha_{\text{critical}}(\mu_{\text{min}}+1)}$.

That is, given μ_{min} of an equilibrium point, the stable and unstable regions are separated by the curve $\gamma_{\text{critical}} = \frac{4-2\alpha_{\text{critical}}}{2-\alpha_{\text{critical}}(\mu_{\text{min}}+1)}$. On the $\gamma - \alpha$ plot, the lower-left side region under the curve is stable while the upper-right region above the curve is unstable.

According to **Propositions** 1 to 3, the stability conditions depend on the minimum eigenvalue of certain Jacobian matrices of the dynamical systems. Below in Table II, we summarize these Jacobian matrices of Weibit-based DTD models derived above in comparsion to those of Logit-based DTD models (which can be found in [8], [14]). Note from Table II that the flow dynamic models and cost dynamic models have the same stability conditions. Also, their fixed points are the same according to the presented **Equivalence conditions** 1 to 3. *Hence, in the later experiments, we only examine the flow dynamic model and the double dynamic model.*

TABLE II: The Jacobian matrices determining the stability of different DTD models under two loading functions.

Model \ loading function	Weibit	Logit
Flow dynamic model	$J_g^{\Phi^{Weibit}} J_f^g$	$J_c^{\Phi^{Logit}} J_f^c$
Cost dynamic model	$J_g^{\Phi^{Weibit}} J_f^g$	$J_c^{\Phi^{Logit}} J_f^c$
Double dynamic model	$J_g^{\Phi^{Weibit}} G J_f^{\ln g}$	$J_c^{\Phi^{Logit}} J_f^c$

5) Comparison of the Jacobian matrices of the two network loading functions: From Table II, the stablity of the DTD models are largely affected by the Jacobian matrices. The Jacobian matrices of the Weibit and Logit-based network loading functions are elaborated below.

$$J_{g,w,ij}^{\Phi,Weibit} = q_w * \begin{cases} -\dfrac{\beta^w g_{w,i}^{-\beta^w}}{g_{w,i}\sum_{i\in W_r} g_{w,i}^{-\beta^w}} + \dfrac{\beta^w g_{w,i}^{-2\beta^w}}{g_{w,i}\left(\sum_{i\in W_r} g_{w,i}^{-\beta^w}\right)^2}, \\ \text{if } i = j, \\ \dfrac{\beta^w g_{w,i}^{-\beta^w} g_{w,j}^{-\beta^w}}{g_{w,j}\left(\sum_{i\in W_r} g_{w,i}^{-\beta^w}\right)^2}, \quad \text{if } i \neq j. \end{cases}$$

$$J_{c,w,ij}^{\Phi,Logit} = q_w * \begin{cases} -\dfrac{\theta e^{-\theta c_{w,i}}}{\sum_{i\in W_r} e^{-\theta c_{w,i}}} + \dfrac{\theta e^{-2\theta c_{w,i}}}{\left(\sum_{i\in W_r} e^{-\theta c_{w,i}}\right)^2}, \\ \text{if } i = j, \\ \dfrac{\theta e^{-\theta c_{w,i}} e^{-\theta c_{w,j}}}{\left(\sum_{i\in W_r} e^{-\theta c_{w,i}}\right)^2}, \quad \text{if } i \neq j. \end{cases}$$

We provide a comparison of the Jacobian matrices of the two network loading functions in Appendix-C.

III. Numerical experiments

We conduct experiments in five networks to demonstrate the Weibit features in the context of DTD dynamics as compared to the Logit-based models. The tested networks and the purpose of each example are summarized in Fig. 2. The travel cost is due to travel time. In Examples 1 and 2, each link is a route, and thus $g = c$, while in other networks, the path travel cost g in the Weibit models is set as $g_{w,r} = e^{\eta c_{w,r}}$, where η is a parameter set as 0.075 ([19], [20]). Example 3 demonstrates the flow dynamic model and double dynamic model, while all other examples demonstrate the flow dynamic model. In Examples 2 to 4, the standard Bureau of Public Roads (BPR) function is used to depict the relationship between travel time and flow, i.e., $t_i = t_i^0\left(1 + a\left(\frac{x_i}{C_i}\right)^b\right)$, where t_i^0 is the free-flow travel time (FFTT) for link i, x_i is the flow of link i, and C_i is the capacity of link i. Parameters a and b are set to 0.15 and 4 respectively. The experiments are coded in Python 3.8 running on a laptop with Intel(R) Core(TM) i7-10510U CPU @ 1.80 GHz, 2.30 GHz and 12.00G RAM.

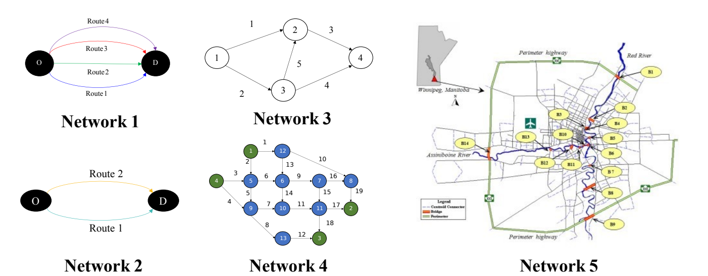

Example (Network)	Network feature	Purpose
1 (A four-route network)	Each link is a route; With multiple routes	Demonstrate the non-identical perception variance feature and how it influences DTD dynamics
2 (A two-route network)	Each link is a route	Demonstrate the stability condition and the feature of asymmetric response curve
3 (Braess network)	A classical network; One route consists of multiple links	Compare the stability regions under various conditions
4 (Nguyen–Dupuis network)	A widely used test network with multiple O-D pairs	Further show the stability region and the non-identical perception variance
5 (Winnipeg network)	A large-scale network	Illustrate the model applicability in real-world transportation networks

Fig. 2: A summary of the used networks, their features and the purposes of the examples

A. Example 1: The non-identical perception error and its impact on the DTD dynamics

This example adopts a four-route single O-D pair network, with the cost functions of Routes 1 to 4 being $t_1 = f_1 + b$, $t_2 = f_2 + b - 5$, $t_3 = f_3 + b - 10$, and $t_4 = f_4 + b - 15$ respectively, where f_i is the flow on the i-th route, and b is a parameter. $q = 20$, $\theta = 0.25$, and $\beta^w = 3.7$.

1) The equilibrium states: We vary the value of parameter b to simulate the length of the networks. The route flows at the equilibrium state of the dynamical systems under different values of b are shown in Fig. 3. It can be observed that in the Logit case, the equilibrium flow patterns remain the same despite the change of b. However, in the Weibit case, the equilibrium flow patterns vary with b, with the flow differences among routes becoming smaller as b increases due to the accordingly growing perception variance. Clearly, the results from the Weibit case should be more reasonable.

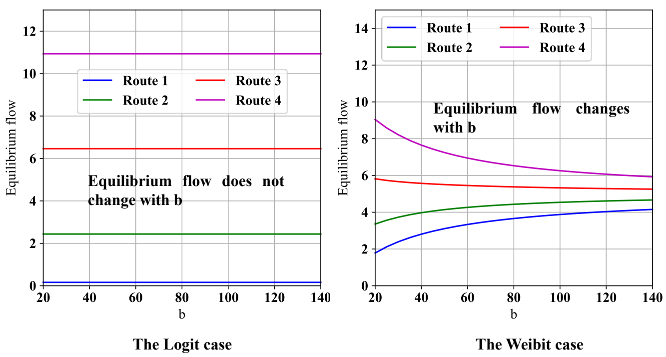

Fig. 3: The route flows at the equilibrium state of Weibit and Logit DTD models under different values of b.

TABLE III: The target flow of each route on day 1 under different models and different values of b

DTD model	Route 1	Route 2	Route 3	Route 4
Weibit, $b = 20$	0.51	1.15	3.35	15
Weibit, $b = 125$	3.94	4.56	5.30	6.2
Logit, $b = 20$	0.34	1.18	4.12	14.37
Logit, $b = 125$	0.34	1.18	4.12	14.37

2) The evolution trajectories: Fig. 4 shows the evolution trajectories of flows and travel times under $b = 20$ and $b = 125$, representing short and long networks respectively, with the initial flow pattern being $(5, 5, 5, 5)$ and $\alpha = 0.1$. From Fig. 4b, in the Logit case, the evolution trajectories of travel times in the long network can be obtained by shifting those in the short network by 105 units of time. Hence, the DTD absolute cost differences between routes in the short network are the same as those in the long network. As a result, in the Logit-based DTD model, the target flow pattern on each day in the short network is the same as that in the long network (See Table III for target flow pattern on day 1 for illustration) since the Logit loading is determined by the absolute difference. So, the flow evolution trajectories are totally the same in the long and short networks in the Logit-based DTD model (see Fig. 4d). In comparison, the flow evolution trajectories of the Weibit-based DTD model in the short and long networks are totally different (see Fig. 4c). The evolution trajectories of the Weibit DTD model should be more reasonable since they capture the non-identical perception variances for trips of different lengths which widely exist in real life (e.g., [33]).

3) The perceived travel time variances: Further, we elaborate on the perceived travel time distributions and travel time variances when $b = 20$. From Fig. 5a and 5c, the variances of travel times of different routes are different in the Weibit model, and even for the same route its variances may vary from one day to another. However, the variances remain the same for different routes in different days in the Logit model (see Fig. 5b and 5d).

B. Example 2: The stability condition and the asymmetric response curve

This example adopts a two-route single O-D pair network with the FFTT of Route 1 and Route 2 set as $t_1^0 = 10$ and $t_2^0 = 15$, capacities set as 10 both, and q set as 20 units, $\theta = 1$ and $\beta^w = 3.7$([19], [20]).

1) The stability condition: We tabulate the process for computing the critical α in Table IV. In this case, the Logit DTD model is locally asymptotically stable for $\alpha < 0.24$ while the Weibit DTD model is stable for $\alpha < 0.72$. Thus, the Weibit DTD model allows a larger range of α for the dynamical system to converge to the equilibrium point than the Logit DTD model. To demonstrate this, we plot the evolution trajectories of the flow of Route 2 under $\alpha = 0.7$ and the initial route flow of (10, 10) in Fig. 6, where it can be found that the Weibit DTD model can converge to the equilibrium state but the Logit DTD model cannot. To analyze in detail, from Table IV, the minimum eigenvalue of the Weibit-based DTD model is larger than that of the Logit-based DTD model (-1.77 versus -7.11). This leads to that the Weibit DTD model has a larger critical α (0.72 versus 0.24). This difference may be attributed to the fact that the matrix $J_c^{\Phi} J_f^c$ of the Logit-based DTD model has a larger norm. Here, the Frobenius norm is calculated as follows: $\sqrt{(-6.32)^2 + (6.32)^2 + (0.126)^2 + (-0.126)^2} = 8.94$ for the Logit case, and $\sqrt{(1.489)^2 + (-1.489)^2 + (0.278)^2 + (-0.278)^2} = 2.14$ for the Weibit case. Thus, the Weibit case is likely to have a larger minimum eigenvalue since smaller norms indicate a less spread in the magnitude of eigenvalues, potentially pushing the minimum eigenvalue higher. The reason for the smaller Frobenius norm in the Weibit case primarily lies in the smaller entries in J_c^{Φ}. Notably, from the 3rd row of Table IV, the entries in $J_c^{\Phi,Logit}$ are approximately 4 times those in $J_c^{\Phi,Weibit}$. This result aligns with Appendix-C.

2) Asymmetric response curve: Asymmetric response curve means that the rates of decreasing/increasing choice probability differ for equal gains/losses of disutility in the Weibit model, which is different from the symmetric response curve in the Logit model ([41]). Here we illustrate this feature in DTD dynamics. We plot the evolution of route choice probability for both models, starting from two extreme flow patterns: (20, 0) and (0, 20), corresponding to cost differences of 41 and

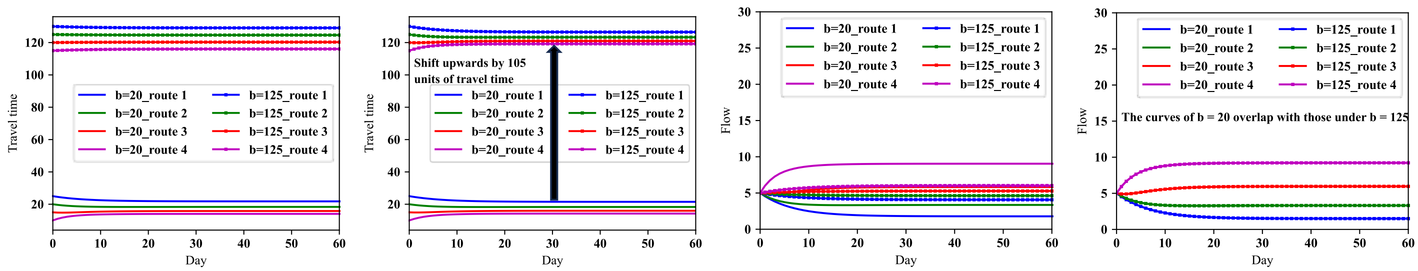

(a) Travel time evolution (Weibit) (b) Travel time evolution (Logit) (c) Flow evolution (Weibit) (d) Flow evolution (Logit)

Fig. 4: The evolution trajectories of travel time and flow under $b = 20$ and $b = 125$

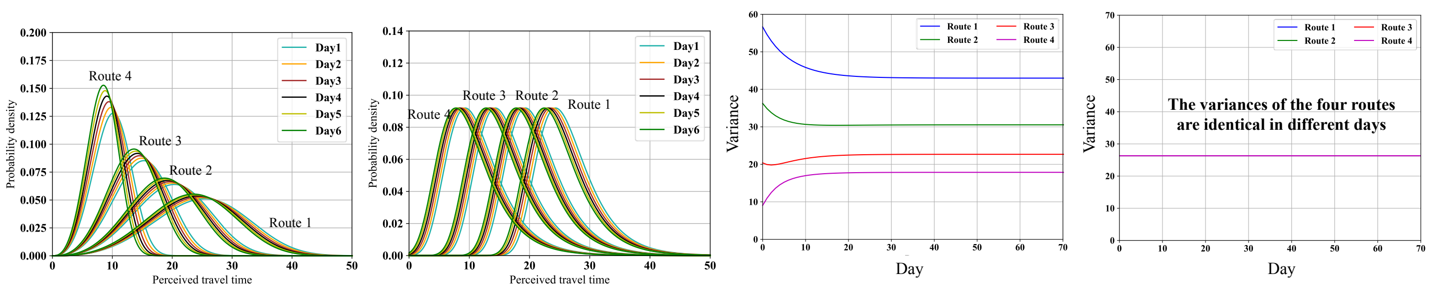

(a) The perceived travel time distribution in the first 6 days (Weibit) (b) The perceived travel time distribution in the first 6 days (Logit) (c) The evolution of travel time variances in the Weibit case (d) The evolution of travel time variances in the Logit case

Fig. 5: The perceived travel time distributions and evolution of travel time variances when $b = 20$

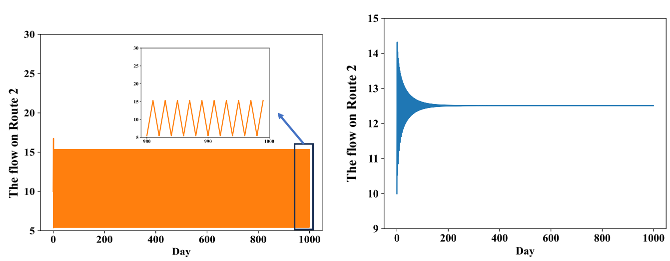

(a) The Logit case (unstable) (b) The Weibit case (stable)

Fig. 6: The flow evolution process of Logit and Weibit flow dynamic models under $\alpha = 0.7$

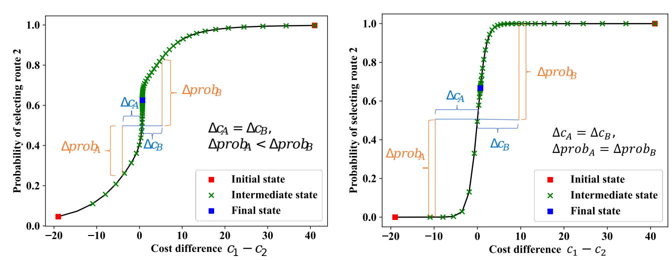

(a) The Weibit case (b) The Logit case

Fig. 7: The evolution of route choice probabilities with respect to cost differences

TABLE IV: The equilibrium states, Jacobian matrices, and critical α of Weibit-based and Logit-based DTD models

	Logit DTD model	Weibit DTD model
Equilibrium flow f^*	$(13.34, 6.66)$	$(12.51, 7.49)$
Equilibrium cost c^*	$(14.75, 15.44)$	$(13.67, 15.71)$
J_c^Φ	$\begin{pmatrix} -4.44 & 4.44 \\ 4.44 & -4.44 \end{pmatrix}$	$\begin{pmatrix} -1.27 & 1.10 \\ 1.27 & -1.10 \end{pmatrix}$
J_f^c	$\begin{pmatrix} 1.424 & 0 \\ 0 & 0.177 \end{pmatrix}$	$\begin{pmatrix} 1.175 & 0 \\ 0 & 0.252 \end{pmatrix}$
$J_c^\Phi J_f^c$	$\begin{pmatrix} -6.32 & 0.126 \\ 6.32 & -0.126 \end{pmatrix}$	$\begin{pmatrix} -1.489 & 0.278 \\ 1.489 & -0.278 \end{pmatrix}$
Minimum eigenvalue	-7.11	-1.77
Critical α	0.24	0.72

-19, respectively. Fig. 7 show the evolution trajectories of the probability of choosing route 2, where each marker represents one day's state. It is observed that the asymmetric/symmetric response features also exist in DTD dynamics and this feature may influence convergence speed (the number of days required to evolve from the initial state to the equilibrium) via the determination of the target flow. Specifically, the initial point with a cost difference of -19 converges slower in the Weibit case compared to the Logit case, while the opposite occurs for the cost difference of 41 since the response curve influences the target flow determination.

C. *Example 3: Stability regions under different conditions*

This example adopts the Braess network, with the FFTT of links 1 to 5 being 2, 2, 2, 3, 1, and their capacities being 4, 7, 7, 4, 3. For fair comparison, except when testing the impact of CoV, the CoV is set as 0.452, which corresponds to $\beta = 3.7$ in the Weibit model and $\theta = 0.57$ in the Logit model.

1) Flow dynamic model: The stability conditions of Logit and Weibit models are compared under different (i) total demand, (ii) network length, and (iii) CoV.

(i) The impact of demand. Under $q = 12, 15$ and 18, the values of critical α are 0.72, 0.36 and 0.2 in the Logit-based DTD model and larger than 1, 0.66, and 0.47 in the Weibit-based DTD model. That is, as q increases, the critical α decreases in both the Logit and Weibit models, indicating a reduction in the stable region. This trend aligns with the findings of [8], which suggest that higher levels of congestion destabilize the system. Notably, the threshold of α is consistently larger in the Weibit DTD model than in the Logit DTD model across the different q levels, indicating that the Weibit equilibrium point possesses a larger stable region.

(ii) The impact of network length. The link free-flow times are scaled by an elongation ratio (er) or increased by an elongation length (el) to simulate network length changes. Under $er = 0.5, 1$, and 2, the values of the critical α are 0.65, 0.36 and 0.2 in the Logit DTD model, and larger than 1, 0.66, and 0.38 in the Weibit DTD model. Under $er = -0.5, 0$, and 0.5, the values of the critical α are 0.5, 0.36 and 0.29 in the Logit DTD model, and 0.83, 0.66, and 0.55 in the Weibit DTD model. Still, the Weibit-SUE has a larger stability region.

(iii) The impact of CoV. The values of θ in the Logit model and β in the Weibit model are varied to test the impact of varying CoV. Under CoV $= 0.35, 0.45$ and 0.55, the critical α values in the Logit-based DTD models are 0.44, 0.36 and 0.30, while being 0.77, 0.66 and 0.54 in the Weibit-based DTD models. That is, increasing CoV (reducing perception error) leads to a decrease in critical α in both models, indicating smaller stable regions. This aligns with [8], suggesting that reducing perception error or increasing shared network knowledge may cause instability. Like before, the Weibit SUE has a larger stability region.

2) Double dynamic model: Unlike the flow dynamic model where critical α can be directly computed, here we compute the $\mu_{\min}$ used to determine the relationship between critical γ and α (recall **Definition 2**). Under $q = 15, 17$, and 19, the values of $\mu_{\min}$ are $-3.03, -5.13$, and -8.16 in the Logit DTD models, while being $-2.01, -3.38$ and -5.37 in the Weibit DTD models. That is, $\mu_{\min}$ is larger in the Weibit case. Hence, the stable region of the Weibit SUE is larger with the critical $\gamma - \alpha$ curve of the Logit model lying to the lower left of that of the Weibit model (See Fig. 8). Also, as demand increases, the critical curve shifts towards the left-lower direction in both models, indicating a shrinkage of the stable region like before.

D. Example 4: Stability region and non-identical perception error in a larger network

This example adopts the 13-node, 19-link and 25-route Nguyen–Dupuis network (see [32]), with $\beta^w = 3.7$ and $\theta = 0.1$ to maintain a comparable CoV.

We first compare the stability conditions of Logit and Weibit DTD models under varying demand. Under $q_w = 200, 300$ and 400 for each O-D pair, the values of critical α are 0.38, 0.11, 0.04 in the Logit case, while being 0.49, 0.29, 0.24 in the Weibit case. As before, the Weibit-based DTD model has

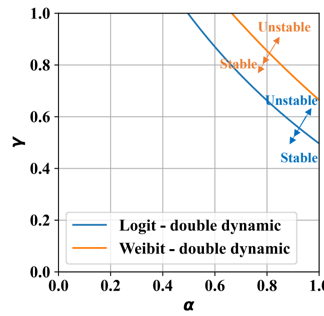

(a) $q = 15$

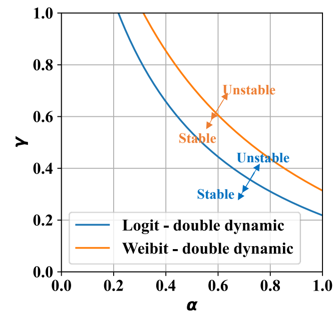

(b) $q = 19$

Fig. 8: The critical $\gamma - \alpha$ curve and the stable/unstable region

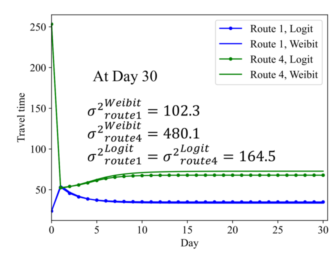

(a) $q_w = 200$, travel time evolution

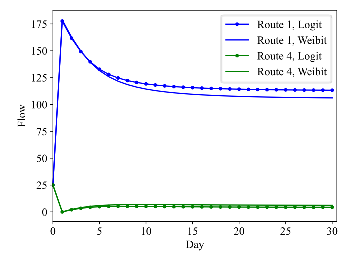

(b) $q_w = 200$, flow evolution

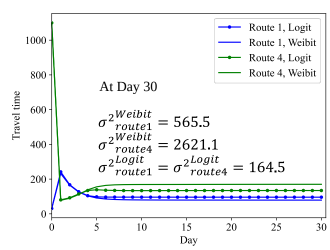

(c) $q_w = 300$, travel time evolution

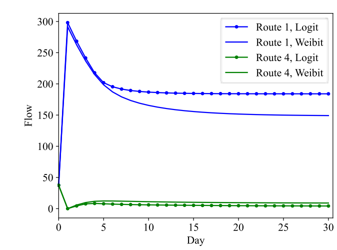

(d) $q_w = 300$, flow evolution

Fig. 9: The evolution of travel times under $q_w = 200$ and 300

consistently larger critical α values, indicating a larger stability region.

Assuming evenly distributed initial route flow, we next examine the evolution process using Route 1 (links $1 \to 10 \to 19$) and Route 4 (links $2 \to 6 \to 14 \to 11 \to 17$) for O–D pair 1, chosen due to their distinct free-flow travel times (22 vs. 45). The flow evolution trajectories (see Figs. 9b and 9d) show that the Weibit model directs more flow to the more congested route (Route 4) at the equilibrium state (similarly, less flow to the less congested Route 1), particularly in the case of $q_w = 300$. Again, this is largely due to that the Weibit model captures the heterogeneous perception variances that the Logit model cannot (see the text in Figs. 9a and 9c). That is, travelers on more congested routes have larger perception variances, leading to higher flow on these routes in the Weibit case than in the Logit case.

E. Example 5: Applicability to the realistic network

We finally show the applicability of the Weibit DTD model in the Winnipeg network with 154 zones, 1067 nodes, 2535 links, 4345 O-D pairs, and adopting a pre-generated route set with 174,491 routes by [42]. The network setting follows [31].

Assuming that the travel demand for each O-D pair is initially evenly distributed across the routes connecting them, we illustrate the evolution of the total system travel time (TSTT, the sum of the products of link flow and link travel time) resulting from the Weibit DTD model under $\alpha = 0.1, 0.2, 0.3$ and 0.4 within 50 days in Fig. 10. Consistent with previous findings, the network equilibrium may get more unstable as α increases, particularly in cases of $\alpha = 0.3$ and 0.4 where the network does not converge to equilibrium.

Under CoV = 0.3, the comparison of the Weibit and Logit DTD models is as follows. (1) The value of critical α is 0.21 in the Weibit case while being 0.18 in the Logit case, further verifying that the Weibit DTD model has a larger stability region in the realistic network. (2) Under $\alpha = 0.17$, it takes 41 and 47 days to reach convergence for Weibit and Logit DTD models respectively. (3) The computation time per iteration (or day) is around 3.1 seconds for both models. (4) After the disruption of Bridge 13, the resilience measure (the ratio of TSTT at the post- and pre-disruption equilibrium) is 1.06 in the Weibit case and 1.01 in the Logit case.

In addition to the above managable computation time, the model can output intermediate results, such as daily route flows and travel times, which can be used to compute DTD network performance measures. Therefore, the Weibit DTD model may support large-scale transportation network analysis (e.g., [31]) and serve as the lower-level model for network design problems in which the consideration of DTD dynamics is necessary (e.g., [30], [43], [44]).

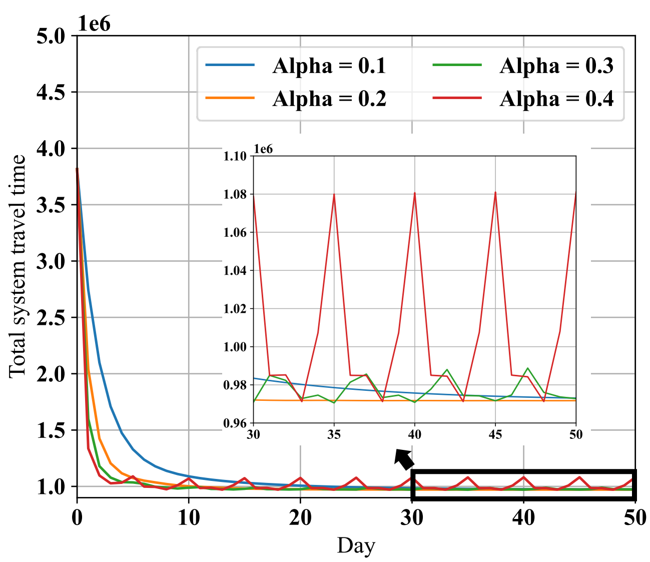

Fig. 10: The evolution of total system travel time under different α in the Winnipeg network

IV. Concluding Remarks and Future Research

The Weibit model offers an ability to capture travelers' heterogeneous perception errors but received limited attention in DTD dynamics. This research makes an initial attempt to systematically examine the Weibit choice model and its features within the context of DTD dynamics.

We present three deterministic discrete Webit DTD models, show the equivalence of their fixed points to Weibit SUE, and provide their local asymptotic stability conditions. We show that accounting for non-identical and day-varying perception variances in Weibit-based DTD models affects the evolution of network states, the equilibrium points, and system stability compared to Logit-based DTD models. The absolute values of the entries in the Jacobian matrix of the Weibit-based loading function tend to be smaller than those in the Jacobian matrix of the Logit-based loading function. As a result, Weibit equilibrium states may correspond to larger minimum eigenvalues in the Jacobian matrix of the dynamical system than Logit equilibrium states. A series of experiments verify that the equilibrium states of Weibit-based DTD models possess larger stable regions of adjustment rates across different conditions under fair comparison. In addition, the feature of the asymmetric response curve in the Weibit model may result in different convergence speed compared to the Logit model where the response curve is symmetric. The applicability of the Weibit DTD model is demonstrated in the Winnipeg network.

Our research has the following practical implications. We demonstrate that the Weibit model effectively accounts for non-identical perception variance in DTD dynamics, resulting in equilibrium states with larger stability regions. With the developed Weibit DTD model and its stability conditions, planners can more accurately capture travelers' route adjustment behaviors and predict how network states may evolve. Moreover, the derived critical adjustment ratios can help determine whether the traffic system can achieve stability or equilibrium after network adjustment. Also, the computation time is manageable. The models and findings can guide the development of more effective transportation planning measures (e.g., new link construction and link protection) or operation strategies (e.g., signal timing and DTD congestion pricing) which lead to more efficient and resilient transportation networks.

Since this research focuses on the theoretical side, real-world calibration work is needed to verify that Weibit choice model can better replicate the DTD dynamics (e.g., [40], [45]). It is also interesting to investigate comparison with AI-driven (e.g., [46], [47]) and UE-based DTD models (e.g., [48]–[50]). The investigated route-based DTD models face challenges in calibration due to the accessibility of route flow data, and future research could explore link-based DTD models (e.g., [11]) which adopt more readily available link flow data.

Appendix

A. Equivalence conditions

1) Flow dynamic model: Below use $*$ to denote the varaible at the equilibrium state. At the fixed point, $f^{k+1} = f^k = f^*$. That is, $\alpha\Phi^{Weibit}(g(f^k)) + (1-\alpha)f^k = f^k$. By manipulation, $f^* = \Phi^{Weibit}(g(f^*))$. This equation defines a self-mapping of the route flow pattern, which coincides with Weibit SUE.

2) Cost dynamic model: At the stable state, $\ln p^* = \ln p^{k+1} = \ln p^k$. By manipulation of Eq. (5), $\ln p^* = \ln g^*(f^*)$, i.e., $p^* = g^*(f^*)$. Substituting it into Eq. (6), we get

$f^* = \Phi^{Weibit}(g^*(f^*))$. This equation defines a self-mapping of the route flow pattern, which coincides with Weibit SUE.

3) Double dynamic model: At the fixed point, $f^{k+1} = f^k = f^*$. By replacing it into Eq. (7), we obtain that $f^* = \Phi_{Weibit}(p(f^*))$. Similarly, $p^{k+1} = p^k = p^*$. By replacing it into Eq. (8), we obtain that $g^* = p^*$. Hence, $f^* = \Phi_{Weibit}(g(f^*))$. This equation defines a self-mapping of the route flow pattern, which coincides with Weibit SUE.

B. Derivation of the stability conditions

1) Flow dynamic model: We examine the local stability of the Weibit-based flow dynamic model (3) + (4) based on the eigenvalue of the dynamical system's Jacobian matrix at the equilibrium state denoted by $J^{Weibit,flow}$. $J^{Weibit,flow} = \alpha J_g^{\Phi^{Weibit}} J_f^g + (1-\alpha)I$, where I is the identity matrix with dimension $N \times N$. The eigenvalues of $J^{Weibit,flow}$, denoted by λ, are the roots of the characteristic equation $|\lambda I - J^{Weibit,flow}| = 0$, where $|J|$ denotes the determinant of matrix J. Combining the formulation of $J^{Weibit,flow}$ and the above characteristic equation, it can be obtained that, $|(\lambda - 1 + \alpha)I - \alpha J_g^{\Phi^{Weibit}} J_f^g| = 0$. Then, each eigenvalue of $J_g^{\Phi^{Weibit}} J_f^g$, denoted by μ_i, corresponds to one eigenvalue of J via the relationship $\lambda - 1 + \alpha - \alpha\mu_i = 0$, i.e., $\lambda(\mu_i) = 1 - \alpha + \alpha\mu_i$. According to [51], for the discrete-time dynamical system, the stability condition requires the moduli of all the eigenvalues of J to be less than 1. That is, $-1 < 1 - \alpha + \alpha\mu_i < 1$. The solution is given by, $1 - \frac{2}{\alpha} < \mu_i < 1$. Note that μ_i is non-positive under mild assumptions of path cost structure and loading function (see [14], [52]), which also holds in the Weibit case. Hence, $\mu_i < 1$ holds automatically. That is, the stability condition only requires for any eigenvalue μ_i of $J_g^{\Phi^{Weibit}} J_f^g$, $\mu_i > 1 - \frac{2}{\alpha}$ holds. This is equivalent to $\mu_{\min} > 1 - \frac{2}{\alpha}$, where $\mu_{\min}$ is the smallest eigenvalue of $J_g^{\Phi^{Weibit}} J_f^g$. This completes the proof.

2) Cost dynamic model: Like before, we write the Jacobian matrix of the dynamical system (5) + (6) at the equilibrium state, denoted by $J^{Weibit,cost}$. Recall that Eq. (5) is $\ln \mathbf{p}^{k+1} = \gamma \ln \mathbf{g}^k(\mathbf{f}^k) + (1-\gamma)\ln\mathbf{p}^k$. Below, we derive the Jacobian matrices of the two terms on the right-hand side. It is easy to see that the second term is $(1-\gamma)I$. We elaborate on the first term below. The partial derivative of $\ln g$ with respect to $\ln p$ is given by $\frac{\partial \ln g}{\partial \ln p} = \frac{(1/g)\partial g}{(1/p)\partial p} = \frac{1/g}{1/p}\frac{\partial g}{\partial f}\frac{\partial f}{\partial p} = \frac{p}{g}\frac{\partial g}{\partial f}\frac{\partial f}{\partial p}$. At the equilibrium state, $p = g$. Hence, $\frac{p}{g} = 1$. That is, $\frac{\partial \ln g}{\partial \ln p} = \frac{\partial g}{\partial f}\frac{\partial f}{\partial p}$. So the first term of the Jacobian matrix of the dynamical system (5) + (6) is $J_g^{\Phi^{Weibit}} J_f^g$. Hence, $J^{Weibit,cost} = \gamma J_g^{\Phi^{Weibit}} J_f^g + (1-\gamma)I$. It can be noted that the only difference between $J^{Weibit,cost}$ and $J^{Weibit,flow}$ lies in that α is replaced by γ. Hence, the stablity condition for the Weibit-based cost dynamic model is given by $\mu_{\min} > 1 - \frac{2}{\gamma}$, where $\mu_{\min}$ is the smallest eigenvalue of $J_g^{\Phi^{Weibit}} J_f^g$. This completes the proof.

3) Double dynamic model: Denote the Jacobian matrix of the Weibit-based double dynamic model (7) + (8) using a block matrix $J^{Weibit,double} = \begin{pmatrix} A_1 & A_2 \\ A_3 & A_4 \end{pmatrix}$. It is easy to show that $A_1 = (1-\gamma)I$ and $A_2 = \gamma J_f^{\ln g}$. We derive A_3 and A_4 below.

A_3 is derived as, $\frac{\partial f^{k+1}}{\partial \ln p^k} = 0 + \alpha \frac{\partial \Phi^{Weibit}}{\partial p^{k+1}} \cdot \frac{\partial p^{k+1}}{\partial \ln p^{k+1}} \cdot \frac{\partial \ln p^{k+1}}{\partial \ln p^k} = \alpha \frac{\partial \Phi^{Weibit}}{\partial p^{k+1}} \cdot p^{k+1}(1-\gamma) \cdot \frac{\partial \ln p^k}{\partial \ln p^k} = \alpha(1-\gamma)\frac{\partial \Phi^{Weibit}}{\partial p^{k+1}} p^{k+1}$. Note at the equilibrium state $p = g$. Hence, A_3 is given by, $A_3 = \alpha(1-\gamma)J_g^{\Phi^{Weibit}} G$ where $G = \text{diag}(g_1, g_2, \ldots, g_N)$.

A_4 is derived as, $\frac{\partial f^{k+1}}{\partial f^k} = (1-\alpha) + \alpha \cdot \frac{\partial \Phi^{Weibit}}{\partial p^{k+1}} \cdot \frac{\partial p^{k+1}}{\partial \ln p^{k+1}} \cdot \frac{\partial \ln p^{k+1}}{\partial f^k} = (1-\alpha) + \alpha \cdot \frac{\partial \Phi^{Weibit}}{\partial p^{k+1}} \cdot p^{k+1} \cdot \gamma \frac{\partial \ln g^k}{\partial f^k}$.At the equilibrium state $p = g$, so A_4 is given by, $A_4 = \alpha\gamma J_g^{\Phi^{Weibit}} G J_f^{\ln g} + (1-\alpha)I$.

To sum up, the Jacobian matrix of the Weibit-based double dynamic model is given by, $J^{Weibit,double} = \begin{pmatrix} (1-\gamma)I & \gamma J_f^{\ln g} \\ \alpha(1-\gamma)J_g^{\Phi^{Weibit}} G & \alpha\gamma J_g^{\Phi^{Weibit}} G J_f^{\ln g} + (1-\alpha)I \end{pmatrix}$

The eigenvalues of $J^{Weibit,double}$, denoted by λ, are the roots of the following characteristic equation, $|\lambda I - J^{Weibit,double}| = 0$, which is equivalent to, $|\left[\lambda - (1-\gamma)\right]\left[\lambda - (1-\alpha)\right] I - \alpha\gamma\lambda J_g^{\Phi^{Weibit}} G J_f^{\ln g}| = 0$ after manipulation.

In comparison, the eigenvalues of $J^{Logit,double}$, denoted by λ, are the roots of the following characteristic equation,$|\left[\lambda - (1-\gamma)\right]\left[\lambda - (1-\alpha)\right] I - \alpha\gamma\lambda J_c^{\Phi^{Logit}} J_f^c| = 0$.

Comparing the above two characteristic equations, it can be found that their difference lies in the last term, which is $J_g^{\Phi^{Weibit}} G J_f^{\ln g}$ in the Weibit case, while it is $J_c^{\Phi^{Logit}} J_f^c$ in the Logit case. Note that in the Logit-based double dynamic model, an equilibrium point is stable when $\mu_{\min} > -2\frac{(1-\gamma)+(1-\alpha)}{\alpha\gamma - 1}$ (see [14]), where $\mu_{\min}$ is the minimum eigenvalue of the matrix $J_c^{\Phi^{Logit}} J_f^c$. Similarly, an equilibrium point of the Weibit-based double dynamical system is stable when $\mu_{\min} > -2\frac{(1-\gamma)+(1-\alpha)}{\alpha\gamma - 1}$, where $\mu_{\min}$ is the minimum eigenvalue of the matrix $J_g^{\Phi^{Weibit}} G J_f^{\ln g}$, and $G = \text{diag}(g_1, g_2, \ldots, g_N)$. This completes the proof.

C. Comparing the Jacobian matrices

Analytically comparing the Jacobian matrices of the Weibit and Logit loading functions is challenging due to the difficulty of explicitly expressing network equilibrium solutions. To explore their differences, we numerically examine a simple two-route network with Jacobian matrices for the Logit and Weibit loading functions (denoted by $J_c^{\Phi^{Logit}}$ and $J_g^{\Phi^{Weibit}}$), each represented by $\begin{bmatrix} j_{11} & j_{12} \\ j_{21} & j_{22} \end{bmatrix}$. We compare the diagonal (j_{11}) and off-diagonal (j_{12}) entries of both matrices, setting $\beta = \theta = 1$ and $q_w = 1$, with hypothesized route costs c_1 and c_2 (or g_1 and g_2) varied from 1 to 10.

Fig. 11 shows contour plots for the Logit, Weibit, and their differences. Figs. 11a and 11d reveal a more complex pattern for Weibit, while Figs. 11b and 11e display the simpler Logit pattern. Focusing on differences, the regions circled in red in Figs. 11c and 11f denote regions where $j_{11}^{Weibit} > j_{11}^{Logit}$ and $j_{12}^{Weibit} < j_{12}^{Logit}$ respectively. Note that in the Jacobian matrices, the off-diagonal entries j_{12} are positive while the diagonal entries j_{11} are negative due to route choice sensitivity (i.e., the probability of choosing a route decreases with its cost while it increases with the costs of all other routes connecting

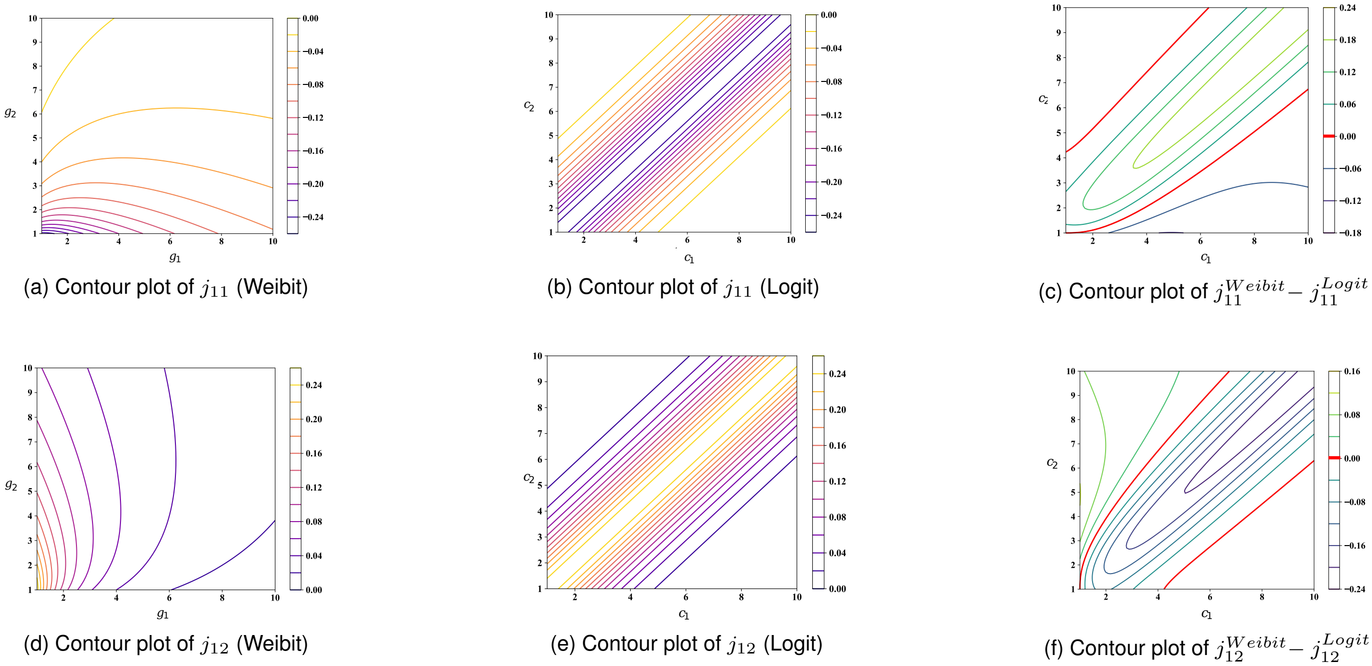

(a) Contour plot of j_{11} (Weibit) (b) Contour plot of j_{11} (Logit) (c) Contour plot of $j_{11}^{Weibit} - j_{11}^{Logit}$

(d) Contour plot of j_{12} (Weibit) (e) Contour plot of j_{12} (Logit) (f) Contour plot of $j_{12}^{Weibit} - j_{12}^{Logit}$

Fig. 11: Comparison of the Jacobian matrices of the two network loading functions

the O-D pair). Also, note that typically, at equilibrium, route cost differences are moderate (i.e., around the 45° diagonal line in Figs. 11c and 11f). Hence, Weibit's Jacobian entries are generally smaller in absolute value than Logit's. This affects the matrix eigenvalues and therefore, stability, as to be discussed in Example 2 at Section III-B.

References

[1] T. Y. Hu and H. S. Mahmassani, "Day-to-day evolution of network flows under real-time information and reactive signal control," *Transportation Research Part C*, vol. 5, no. 1, pp. 51–69, 1997.

[2] H. Ye and H. Yang, "Continuous price and flow dynamics of tradable mobility credits," *Transportation Research Part B*, vol. 57, pp. 436–450, 2013.

[3] R. Y. Guo and H. J. Huang, "Day-to-day dynamics in a duopoly ride-sourcing market," *Transportation Research Part C*, vol. 135, p. 103528, 2022.

[4] R. Zhong, Q. Liang, D. Xu, M. Smith, and T. Pan, "Day-to-day road pricing and network performance analysis via output stability," *IEEE Transactions on Intelligent Transportation Systems*, 2024.

[5] M. J. Beckmann, C. B. McGuire, and C. B. Winsten, *Studies in the Economics of Transportation*. New Haven, Connecticut: Yale University Press, 1956.

[6] H.-J. Cho and M.-C. Hwang, "A stimulus-response model of day-to-day network dynamics," *IEEE Transactions on Intelligent Transportation Systems*, vol. 6, no. 1, pp. 17–25, 2005.

[7] J. L. Horowitz, "The stability of stochastic equilibrium in a two-link transportation network," *Transportation Research Part B*, vol. 18, no. 1, pp. 13–28, 1984.

[8] G. E. Cantarella and E. Cascetta, "Dynamic processes and equilibrium in transportation networks: towards a unifying theory," *Transportation Science*, vol. 29, no. 4, pp. 305–329, 1995.

[9] D. Watling, "Stability of the stochastic equilibrium assignment problem: a dynamical systems approach," *Transportation Research Part B*, vol. 33, no. 4, pp. 281–312, 1999.

[10] J. Bie and H. K. Lo, "Stability and attraction domains of traffic equilibria in a day-to-day dynamical system formulation," *Transportation Research Part B*, vol. 44, no. 1, pp. 90–107, 2010.

[11] R. Y. Guo, H. Yang, and H. J. Huang, "A discrete rational adjustment process of link flows in traffic networks," *Transportation Research Part C*, vol. 34, pp. 121–137, 2013.

[12] M. J. Smith and D. P. Watling, "A route-swapping dynamical system and lyapunov function for stochastic user equilibrium," *Transportation Research Part B*, vol. 85, pp. 132–141, 2016.

[13] L. Xiao and H. K. Lo, "Combined route choice and adaptive traffic control in a day-to-day dynamical system," *Networks and Spatial Economics*, vol. 15, pp. 697–717, 2015.

[14] H. Ye, F. Xiao, and H. Yang, "Day-to-day dynamics with advanced traveler information," *Transportation Research Part B*, vol. 144, pp. 23–44, 2021.

[15] H. Ye, "On stochastic-user-equilibrium-based day-to-day dynamics," *Transportation Science*, vol. 56, no. 1, pp. 103–117, 2022.

[16] R. B. Dial, "A probabilistic multipath traffic assignment model which obviates path enumeration," *Transportation Research*, vol. 5, no. 2, pp. 83–111, 1971.

[17] C. Fisk, "Some developments in equilibrium traffic assignment," *Transportation Research Part B*, vol. 14, no. 3, pp. 243–255, 1980.

[18] E. Castillo, J. M. Menéndez, P. Jiménez, and A. Rivas, "Closed form expressions for choice probabilities in the weibull case," *Transportation Research Part B*, vol. 42, no. 4, pp. 373–380, 2008.

[19] S. Kitthamkesorn and A. Chen, "Path-size weibit stochastic user equilibrium model," *Transportation Research Part B*, vol. 57, pp. 378–397, 2013.

[20] S. Kitthamkesorn and A. Chen, "Unconstrained weibit stochastic user equilibrium model with extensions," *Transportation Research Part B*, vol. 59, pp. 1–21, 2014.

[21] M. Fosgerau and M. Bierlaire, "Discrete choice models with multiplicative error terms," *Transportation Research Part B*, vol. 43, no. 5, pp. 494–505, 2009.

[22] F. Kurauchi and H. Ido, "Estimation of the expressway/surface road choice model using logit-weibit hybrid model," in *Proceedings of the 22nd International Conference of Hong Kong Society for Transportation Studies (HKSTS)*, (Hong Kong), 2017.

[23] D. Li, W. Wu, and Y. Song, "Comparative study of logit and weibit model in travel mode choice," *IEEE Access*, vol. 8, pp. 63452–63461, 2020.

[24] K. Wen, J. Xie, A. Chen, S. C. Wong, S. Zhan, S. M. Lo, and L. Qiang, "Empirical analysis of scaled mixed itinerary-size weibit model for itinerary choice in a schedule-based railway network," *Transportmetrica A: Transport Science*, vol. 18, no. 3, pp. 934–962, 2022.

[25] Y. Gu, A. Chen, and S. Kitthamkesorn, "Modeling shared parking services at spatially correlated locations through a weibit-based combined destination and parking choice equilibrium model," *Transportation Research Part B*, vol. 186, p. 103000, 2024.

[26] Y. Gu and A. Chen, "Modeling mode choice of customized bus services with loyalty subscription schemes in multi-modal transportation networks," *Transportation Research Part C*, vol. 147, p. 104012, 2023.
[27] Y. Gu, A. Chen, S. Kitthamkesorn, and S. Jang, "Alternate closed-form weibit-based model for assessing travel choice with an oddball alternative," *Transportation Research Part B*, vol. 179, p. 102867, 2024.
[28] S. Kitthamkesorn, A. Chen, S. Ryu, and S. Opasanon, "Maximum capture problem based on paired combinatorial weibit model to determine park-and-ride facility locations," *Transportation Research Part B*, vol. 179, p. 102855, 2024.
[29] J. S. W. J. Xie, S. C. Wong, S. Zhan, S. M. Lo, and A. Chen, "Train schedule optimization based on schedule-based stochastic passenger assignment," *Transportation Research Part E*, vol. 136, p. 101882, 2020.
[30] K. Qu, X. Xu, and A. Chen, "Static congestion pricing considering the cumulative impact of day-to-day dynamics with weibit adjustment process," *Transportmetrica B: Transport Dynamics*, vol. 10, no. 1, pp. 237–265, 2022.
[31] X. Xu, K. Qu, A. Chen, and C. Yang, "A new day-to-day dynamic network vulnerability analysis approach with weibit-based route adjustment process," *Transportation Research Part E*, vol. 153, p. 102421, 2021.
[32] B. Zhou, M. Xu, Q. Meng, and Z. Huang, "A day-to-day route flow evolution process towards the mixed equilibria," *Transportation Research Part C*, vol. 82, pp. 210–228, 2017.
[33] Y. Sheffi, *Urban Transportation Network*. Prentice Hall, 1985.
[34] E. Cascetta, "A stochastic process approach to the analysis of temporal dynamics in transportation networks," *Transportation Research Part B*, vol. 23, no. 1, pp. 1–17, 1989.
[35] T. Iryo, D. Watling, and M. Hazelton, "Estimating markov chain mixing times: Convergence rate towards equilibrium of a stochastic process traffic assignment model," *Transportation Science*, 2024.
[36] M. J. Smith, "The stability of a dynamic model of traffic assignment – an application of a method of lyapunov," *Transportation Science*, vol. 18, no. 3, pp. 259–304, 1984.
[37] T. Friesz, D. Bernstein, N. Mehta, R. Tobin, and S. Ganjalizadeh, "Day-to-day dynamic disequilibria and idealized traveller information systems," *Operations Research*, vol. 42, no. 6, pp. 1120–1136, 1994.
[38] D. Zhang and A. Nagurney, "On the local and global stability of a travel route choice adjustment process," *Transportation Research Part B*, vol. 30, no. 4, pp. 245–262, 1996.
[39] F. Yang and D. Zhang, "Day-to-day stationary link flow pattern," *Transportation Research Part B*, vol. 43, no. 1, pp. 119–126, 2009.
[40] Q. Cheng, S. Wang, Z. Liu, and Y. Yuan, "Surrogate-based simulation optimization approach for day-to-day dynamics model calibration with real data," *Transportation Research Part C*, vol. 105, pp. 422–438, 2019.
[41] Y. Gu, A. Chen, and S. Kitthamkesorn, "Weibit choice models: Properties, mode choice application and graphical illustrations," *Journal of Choice Modelling*, vol. 44, p. 100373, 2022.
[42] S. Bekhor, L. Reznikova, and T. Toledo, "Application of cross-nested logit route choice model in stochastic user equilibrium traffic assignment," *Transportation Research Record*, vol. 2003, no. 1, pp. 41–49, 2007.
[43] Z. Liu, S. Wang, B. Zhou, and Q. Cheng, "Robust optimization of distance-based tolls in a network considering stochastic day to day dynamics," *Transportation Research Part C*, vol. 79, pp. 58–72, 2017.
[44] R. Yin, Z. Liu, and N. Zheng, "A simulation-based model for continuous network design problem using bayesian optimization," *IEEE Transactions on Intelligent Transportation Systems*, vol. 23, no. 11, pp. 20352–20367, 2022.
[45] H. Qi, N. Jia, X. Qu, and Z. He, "Investigating day-to-day route choices based on multi-scenario laboratory experiments, part i: Route-dependent attraction and its modeling," *Transportation Research Part A*, vol. 167, p. 103553, 2023.
[46] M. Owais, "Deep learning for integrated origin–destination estimation and traffic sensor location problems," *IEEE Transactions on Intelligent Transportation Systems*, 2024.
[47] L. Wang, P. Duan, Z. He, C. Lyu, X. Chen, N. Zheng, L. Yao, and Z. Ma, "Ai-driven day-to-day route choice," *arXiv*, vol. 2412, 2024.
[48] E. Castillo, J. M. Men'endez, and S. S'anchez-Cambronero, "Traffic estimation and optimal counting location without path enumeration using bayesian networks," *Computer-Aided Civil and Infrastructure Engineering*, vol. 23, no. 3, pp. 189–207, 2008.
[49] M. Owais and A. E. Matouk, "A factorization scheme for observability analysis in transportation networks," *Expert Systems with Applications*, vol. 174, p. 114727, 2021.
[50] J. Li, Z. Wang, and Y. Nie, "Wardrop equilibrium can be boundedly rational: A new behavioral theory of route choice," *Transportation Science*, vol. 58, no. 5, pp. 973–994, 2024.
[51] H. K. Khalil, *Nonlinear Systems*. Upper Saddle River, NJ: Prentice Hall, 3rd ed., 2002.
[52] F. Zhang, *Matrix Theory: Basic Results and Techniques*. New York: Springer, second ed., 2011.

Kai Qu is a PhD candidate at the Hong Kong Polytechnic University and Tongji University. His research interests include network reliability, vulnerability, resilience, and day-to-day dynamics. His work has been published in ISTTT, Transportation Research Part B/C/E.

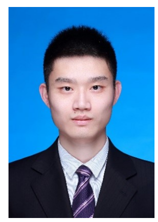

Yu Gu received his Ph.D. from the Department of Civil and Environmental Engineering, Hong Kong Polytechnic University, where he is currently a postdoctoral fellow. His research interests include the transportation network equilibrium model, random utility model, and network reliability, vulnerability, and resilience. His work has been published in Transportation Research Part B/C/E, Communications in Transportation Research, Journal of Choice Modelling.

Zhaoqi Zang is a PhD student at Nanyang Technological University, Singapore. He obtained his bachelor's degree and master's degree from Tongji University, China. His research interests include time risk and reliability, network modelling and optimization. His work has been published in ISTTT and Transportation Research Part B/C/E, and IEEE-TITS.

Anthony Chen is a Professor and Associate Head in the Department of Civil and Environmental Engineering at the Hong Kong Polytechnic University. He received the NSF Career Award and was the Chang Jiang Chair Professor at Tongji University. With over 10,000 Google Scholar citations, he serves as an Associate Editor for Transportmetrica A and Networks & Spatial Economics and is an editorial board member of Transportation Research Part B. His research interests include transportation network modeling and analysis.

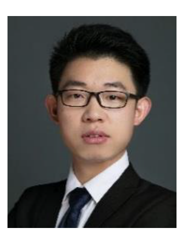

Xiangdong Xu is currently a Professor with the College of Transportation Engineering, Tongji University, Shanghai, China. His research interests include transportation network modeling and optimization, transportation system resilience analysis, network flow estimation and sensors location, and shared and connected transportation systems.